ChemPubSoc Europe

DOI: 10.1002/chem.201304380

CHEMISTRY A European Journal Full Paper

Molecular Tweezers

Dynamic Properties of Molecular Tweezers with a Bis(2-hydroxyphenyl)pyrimidine Backbone

Yoshitaka Tsuchido,[a] Yuji Suzaki,[a] Tomohito Ide,[a, b] and Kohtaro Osakada*[a]

Abstract: 4,6-Bis(2-hydroxyphenyl)-2-alkylpyrimidines with two anthryl or 9-ethylnylanthryl substituents at the positions *para* to the OH groups prefer a U-shaped conformation supported by two intramolecular OH···N hydrogen bonds in the solid state and in $CDCl_3$ solution. The compound with a hexyl substituent on the pyrimidine group and two 9-ethynylanthryl arms at the hydroxyphenyl groups forms a 1:1 complex with 2,4,7-trinitrofluorenone. Its association constant K_a was estimated to be 2100 M^{-1} at 298 K, which is larger than those of other molecular tweezers ($K_a <$ 1000 M^{-1}). DFT calculations suggested that the complex adopts a stable conformation supported by intramolecular hydrogen bonds among the OH groups and the pyrimidine ring as well as by intermolecular π–π interaction between the anthryl groups and 2,4,7-trinitrofluorenone. Addition of nBu$_4$NF to a solution of the molecular tweezers or their complexes causes the cleavage of one or two OH···N hydrogen bonds, formation of new O···HF hydrogen bonds, and changes in the molecular conformation. The resulting structure of the molecular tweezers contains nonparallel anthryl groups, which do not bind the guest molecule. Photochemical measurements on 4,6-bis(2-hydroxyphenyl)-2-methylpyrimidine with two anthryl substituents showed negligible luminescence (quantum yield $\phi < 0.01$), owing to photoinduced electron transfer of the molecule with a U-shaped structure. However, the *O*-hexylated compound exhibits emission from the anthryl groups with $\phi = 0.39$.

Introduction

The history of host–guest chemistry dates back to the discovery of cyclic host molecules that bind guest molecules efficiently.[1] In 1978, Whitlock et al. reported a complex of aromatic carboxylic acids with an acyclic host composed of two caffeine groups connected by a polymethylene spacer.[2] The interaction between the guest molecule and the aromatic functional groups of the host stabilizes the complex, and a more directional interaction than that of complexes of cyclic hosts is required for stoichiometric aggregation. Acyclic host compounds of this type were proposed as molecular tweezers.[3] Zimmerman et al. designed such host compounds containing two anthracene groups separated by a rigid spacer and reported their complexation of many aromatic guests and applications, such as the selective recognition of nucleobases and the separation of polyaromatic hydrocarbons.[4] Guests in such complexes include planar organic molecules or their π-conjugated parts,[5] planar transition metal complexes,[6] fullerenes,[7] carbon nanotubes,[8] and crown ether and dialkyl ammonium pseudorotaxanes.[9] Host molecules whose stable conformation does not have a cavity that allows for complexation were also reported to bind guest molecules on their structural change. Klärner et al. prepared a host compound in which anthracene groups are arranged in a nonparallel orientation because of the spacer structure; the conformation becomes parallel on forming a complex with an aromatic guest.[10] Similar induced-fit conformational changes are observed for various host–guest combinations.[11] A compulsory structural change of bifunctional compounds is induced in a molecular motor.[12]

Lehn designed unsymmetrical host compounds and demonstrated complexation of a guest molecule induced by outer stimulation.[13] The addition of transition metal ions to terpyridine with two anthracene groups in the *meta* positions changes its open conformation to a U-shaped one by the chelation of the terpyridine group to the metal centers.[14] Two parallel terminal anthryl groups bind planar aromatic guest molecules. This system enables reversible catching and release of organic guests by repeated cycles of coordination and decoordination of the transition metals. Jang et al. reported allosteric molecular tweezers whose binding of an organic guest is highly influenced by the chloride anion.[15] Saint-Aman, Bucher et al. designed redox-responsive porphyrin-based molecular tweezers.[16] Petitjean, Leroux et al. employed 2,6-diarylpyridine as the spacer for the naphthalene moieties of their molecular tweezers and showed its pH-dependent behavior based on their conformational change.[17] As shown in Scheme 1 a, the

[a] *Y. Tsuchido, Dr. Y. Suzaki, Dr. T. Ide, Prof. Dr. K. Osakada*
Chemical Resources Laboratory, Tokyo Institute of Technology
4259 R2-3, Nagastuta, Midori-ku, Yokohama 226-8503 (Japan)
Fax: (+81) 45-924-5224
E-mail: kosakada@res.titech.ac.jp

[b] *Dr. T. Ide*
Present address: Corporate Research and Development Center
Toshiba Corporation
1, Komukai-Toshiba-cho, Saiwai-ku, Kawasaki 212-8582 (Japan)

Supporting information for this article is available on the WWW under http://dx.doi.org/10.1002/chem.201304380.

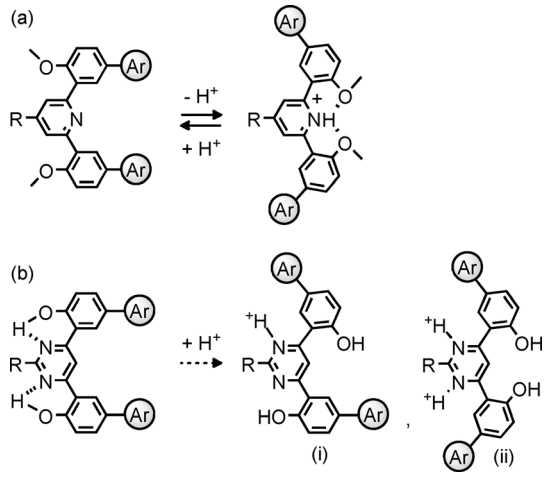

Scheme 1. Conformational change of backbone structures by addition of acid or base. a) 2,6-Diarylpyridine[17] and b) bis(2-hydroxyphenyl)pyrimidine.[18]

molecule adopts an open conformation under non-acidic conditions, and the addition of protic acid gives it a pinched structure. Recently, we reported bis(hydroxyphenyl)pyrimidine derivatives and their different conformations depending on their substituents.[18] Bis(hydroxyphenyl)pyrimidine has a U-shaped structure stabilized by OH···N hydrogen bonds (Scheme 1b). The addition of a proton to a pyrimidine nitrogen atom forms a molecule with an S-shaped conformation (Scheme 1bi), whereas protonation of both nitrogen atoms yields a W-shaped molecule (Scheme 1bii). The use of F^- instead of H^+ was expected to cause a clear structural change, because Dai and Zhao have recently reported cleavage of the OH···N hydrogen bond of polyaromatic compounds caused by the addition of F^-.[19] Herein, we present the preparation, structure, and stimulation-dependent properties of 4,6-pyrimidine-based molecular tweezers.

Results and Discussion

Preparation and structure of molecular tweezers

Figure 1 shows the host molecules used in this study. Compounds **1-OH** and **2-OH** with two anthrylalkynyl groups bonded to 4,6-bis(2-hydroxyaryl)pyrimidine were prepared by a combination of cross-coupling reactions involving organomagnesium and organoboron compounds. Compound **3-OH** without an alkynyl group was prepared in accordance with a previous report.[18]

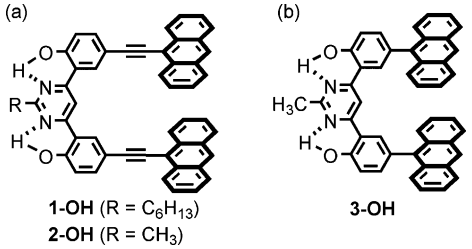

Figure 1. Structures of molecular tweezers with bis(2-hydroxylphenyl)pyrimidine backbone. a) **1-OH** and **2-OH**. b) **3-OH**.

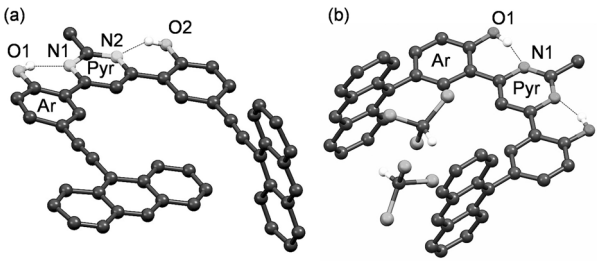

Figure 2. Crystal structures of molecular tweezers (ball-and-stick representation). a) **2-OH** and b) **3-OH**·2$CHCl_3$.[18] The OH hydrogen atoms of **2-OH** were calculated by assuming OH···N hydrogen bonds. Dashed lines indicate OH···N hydrogen bonds.

The structure of **2-OH** determined by X-ray crystallography is compared with that of **3-OH**[18] in Figure 2. Molecules of **2-OH** and **3-OH**·2$CHCl_3$ have small dihedral angles between the pyrimidyl (Pyr) and arene (Ar) rings ($\measuredangle$Ar–Pyr = 5.3 and 1.4°, respectively). The difference Fourier synthesis of **3-OH**·2$CHCl_3$ revealed the position of the OH hydrogen atoms with H···N distances of 1.75 Å, whereas the crystallographic study on **2-OH** did not provide information on the position of OH hydrogen atoms. The coplanarity of the three aromatic rings and the close contact of the O and N atoms (2.54 and 2.56 Å) of **2-OH**, however, suggest hydrogen bonds. The IR spectra of **2-OH** and **3-OH**·2$CHCl_3$ (KBr disk) show broad ν(OH) peaks at 2550 and 2710 cm^{-1}, which also indicate OH···N hydrogen bonds. The anthracene planes of **2-OH** are tilted by 72.0° (Figure 2a). A C–H···π interaction[20] exists between the anthryl proton and the π surface. However, **3-OH**·2$CHCl_3$ has two $CHCl_3$ molecules of solvation, which are intercalated between the two parallel anthracene planes (Figure 2b). The C–H···π interaction of $CHCl_3$ with anthryl groups serves to maintain the conformation with parallel anthracene planes. Yam et al. designed OH-free bis-aryl pyridine-type molecular tweezers with two square-planar Pt complexes at the end of the two arms to maintain its conformation.[21]

We compared the structures of the above molecular tweezers with those of *O*-alkylated derivatives. Hexylation of the OH groups of **2-OH** and **3-OH** produced compounds **2-OHex** and **3-OHex** (Scheme 2).[18] X-ray structure determination revealed

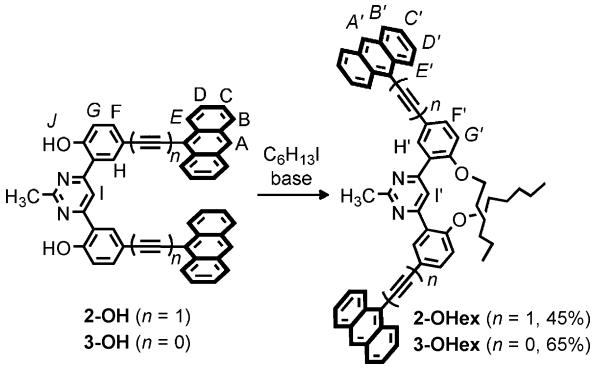

Scheme 2. Synthesis of *O*-alkylated bis(2-hydroxyphenyl)pyrimidines **2-OHex** and **3-OHex**.

W-shaped conformations with dihedral angles between the arylene (Ar) and pyrimidine (Pyr) rings of 26.4° (**2-OHex**) and 40.0, 30.6° (**3-OHex**). CH···O interactions (2.32 Å in **2-OHex**; 2.40 and 2.32 Å in **3-OHex**) between oxygen and pyrimidinyl hydrogen atoms were noted.

The ^{1}H NMR spectra of **3-OH** and **3-OHex** are compared in Figure 3. The ^{1}H NMR spectrum of **3-OH** shows a broad signal for an OH hydrogen atom (H_j) at a much lower field ($\delta_H =$ 14.01) than typical OH groups due to the intramolecular OH···N hydrogen bonds between hydroxyl hydrogen and pyrimidinyl nitrogen atoms. This signal suggests that **3-OH** maintains its U-shaped conformation in $CDCl_3$ solution, as well as in the solid state (Figure 2b). Stueber et al. reported similar intramolecular OH···N hydrogen bonds in 2,4-bis(2′-hydroxyaryl)-1,3,5-triazine (δ_H(OH) = 13.2).[22] The ^{1}H NMR signal of the pyrimidinyl hydrogen atom of **3-OHex** (H_i, $\delta_H = 8.51$ ppm) was observed at a lower field than that of **3-OH** ($\delta_H = 7.85$ ppm), which is attributed to the CH···O interaction of the former compound with a W-shaped conformation in $CDCl_3$. The above results are consistent with the notion that the conformations of **3-OH** and **3-OHex** are stabilized by OH···N and CH···O hydrogen bonds in both $CDCl_3$ solution and the solid state.

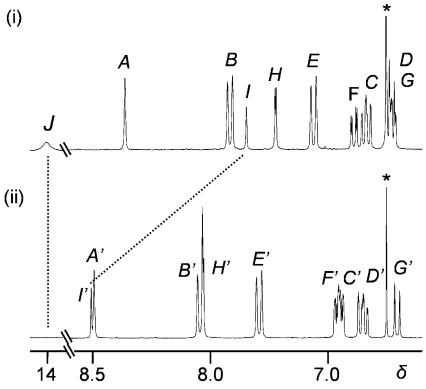

Figure 3. ^{1}H NMR spectra of i) **3-OH** and ii) **3-OHex** ($CDCl_3$, 400 MHz, 298 K). See Scheme 2 for assignments of the signals.

Host–guest complexation of molecular tweezers and guest molecules

Complexation of molecular tweezers **1-OH** and **3-OH** with guest molecules 2,4,7-trinitrofluorenone (TNF), 1,2,4,5-tetracyanobenzene (TCB), and tetracyanoquinodimethane (TCNQ) was investigated by UV/Vis spectroscopy, ^{1}H NMR titration, and DFT calculations.

In $CDCl_3$, **1-OH** and TNF formed inclusion complex **1-OH**⊃TNF, as shown in Scheme 3. The addition of a colorless solution of TNF to a yellow solution of **1-OH** (1.0 mmol L^{-1} $CHCl_3$) resulted in a brown solution, suggesting interaction between the anthryl groups of **1-OH** and TNF. Decreased absorbance of **1-OH** (0.050 mmol L^{-1}) at 430 nm, assigned to the π–π* transition of anthryl groups, was accompanied by the growth of a new broad peak at 460–550 nm

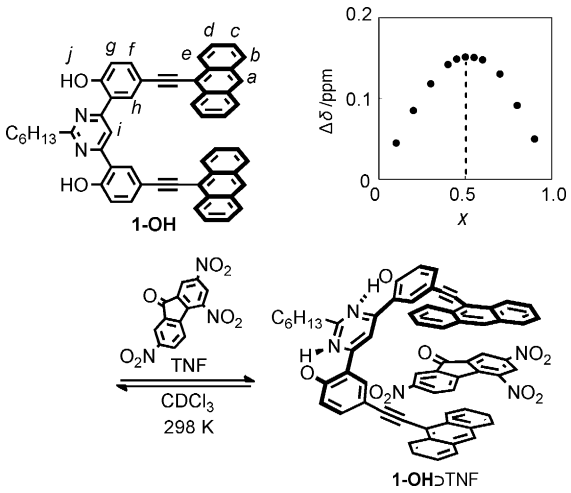

Scheme 3. Complexation of molecular tweezers **1-OH** with TNF to form **1-OH**⊃TNF. Inset: Job plot of **1-OH** and TNF determined by ^{1}H NMR titration ($CDCl_3$, [**1-OH**] + [TNF] = 1.0 mmol L^{-1}, 298 K).

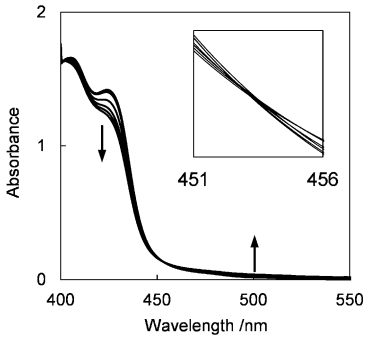

Figure 4. UV/Vis monitoring of the titration of a solution of **1-OH** ($CHCl_3$, [**1-OH**] = 0.050 mmol L^{-1}, 298 K) with TNF. The inset shows the isosbestic point at 453 nm.

(Figure 4). Observation of an isosbestic point at 453 nm indicated formation of a single complex from **1-OH** and TNF.

The addition of TNF to a solution of **1-OH** in $CDCl_3$ ([**1-OH**] = 1.0 mmol L^{-1}) also changed the ^{1}H NMR spectrum. An upfield shift of anthryl protons (H_a, H_b, H_c, H_d, H_e), phenyl protons (H_f, H_g), and a hydroxyl proton (H_j), as well as a downfield shift of the pyrimidine proton (H_i) and TNF protons were noted. The peak of H_a was shifted from $\delta_H = 8.41$ ppm ([**1-OH**] = 1.0 mmol L^{-1}, [TNF] = 0.0 mmol L^{-1}) to 7.79 ppm ([TNF] = 20.0 mmol L^{-1}). These shifts are explained by the charge-transfer (CT) interaction between the anthryl groups of **1-OH** and electron-deficient TNF. The CT should cause upfield shifts of electron-rich anthryl protons and downfield shifts of the electron-deficient TNF protons. A Job plot for **1-OH** and TNF, obtained by ^{1}H NMR titration in $CDCl_3$ at 298 K ([**1-OH**] + [TNF] = 1.0 mmol L^{-1}), showed a peak maximum at a mole fraction of 0.5 (Scheme 3, inset), which indicates formation of 1:1 inclusion complex **1-OH**⊃TNF between **1-OH** and TNF.

The association constant K_a of complex formation was estimated to be 2100 M^{-1} ($CDCl_3$, 298 K) from a Scatchard plot obtained on the basis of the shift of an anthryl proton (H_a). It is

larger than that of molecular tweezers with a rigid dibenzo-[*c*,*h*]acridine backbone unit ($K_a = 1000\ M^{-1}$, $CHCl_3$, 298 K) reported by Zimmerman et al.[4] The high affinity of **1-OH** for TNF is due to the two following reasons. The OH···N hydrogen bonds between the pyrimidinyl nitrogen and hydroxyl hydrogen atoms allow for adjustment of the conformation of the bis-anthryl pyrimidine backbone, so that the anthryl groups are situated in a position optimal for squeezing the guest molecule. Ethynylene spacers between the backbone and the anthryl groups form a cavity suitable for large guest molecules. The thermodynamic parameters of this reaction were calculated to be $\Delta G^\circ = -19.0\ kJ\,mol^{-1}$, $\Delta H^\circ = -29.4\ kJ\,mol^{-1}$, and $\Delta S^\circ = -35\ J\,mol^{-1}\,K^{-1}$. The large negative ΔH and ΔS imply intermolecular complex formation driven by the attractive interaction between **1-OH** and TNF.

The association constants K_a of the complexation of **1-OH** and **3-OH** with TNF, TCB, and TCNQ are listed in Table 1. Molecular tweezers **1-OH** showed association constants of $2100\ M^{-1}$ for TNF, $530\ M^{-1}$ for TCB, and $93\ M^{-1}$ for TCNQ. **3-OH** has a low affinity to TNF ($K_a = 300\ M^{-1}$) and undergoes negligible complex formation with TCB and TCNQ. The difference in affinity between **1-OH** and **3-OH** to the electron-deficient guests can be attributed to the size of the cavity for guest binding. The anthracene units of **3-OH** are bonded directly to aromatic rings, which are perpendicular to the anthracene plane. As shown in Figure 2b, the C–H groups of the aromatic rings narrow the cavity for the guest molecules. In contrast, **1-OH** has a large cavity for guest binding and allows for a strong interaction between the anthracene units and the guest molecule. The negatively charged π surface of TNF due to electron-withdrawing nitro groups causes a strong CT interaction with two anthracene units of the molecular tweezers. The K_a values of the *O*-alkylated compounds **2-OHex** and **3-OHex** with the guest molecules (TNF, TCNQ, and TNF) are negligible ($K_a < 40\ M^{-1}$, $CDCl_3$, 298 K) owing to their unfavorable conformations for guest binding.

Table 1. Association constants of complex formation.

Molecular tweezers	Guest	Association constant K_a [M^{-1}][a]
1-OH	TNF	2100
	TCB	550
	TCNQ	93
3-OH	TNF	300
	TCB	<1
	TCNQ	<1

[a] Determined by ^1H NMR titration (Scatchard plot), $CDCl_3$, [molecular tweezers] = 1.0 mmol L^{-1}, 298 K.

The interactions of **1-OH** and TNF were studied in detail by DFT calculations. Figure 5a and b show two plausible conformations of the inclusion complex **1-OH**⊃TNF (i.e., $Conf_1$ and $Conf_2$, respectively), which differ in the orientation of the TNF molecule in the cavity of **1-OH**. In $Conf_1$, the carbonyl oxygen atom of TNF is hydrogen-bonded to the pyrimidine ring of **1-OH**, whereas in $Conf_2$ the TNF guest is stabilized by interaction of an NO_2 group of TNF with the pyrimidine CH group and in the opposite direction to that in $Conf_1$. Both structures were optimized by DFT calculation (B97-D/TZVP). The calculated relative free energies suggested higher stability of $Conf_1$ than $Conf_2$ by $\Delta G = -6.3\ kJ\,mol^{-1}$. The interaction between the carbonyl oxygen atom of TNF and the acidic hydrogen atom is effective for the stabilization of $Conf_1$. The downfield shift of the ^1H NMR peak of the pyrimidyl proton (H_i) is explained by the interaction with the carbonyl oxygen atom of TNF with the conformation $Conf_1$, as shown in Figure 5a. The molecular orbitals of $Conf_1$ were also obtained by DFT calculation. The HOMO and its degenerate orbital HOMO−1 are extended over the anthracene rings and phenyl groups of **1-OH**, whereas the LUMO is localized on TNF. The Mülliken charges of **1-OH** and TNF were calculated to be positive (+0.096) and negative (−0.096), respectively, and thus indicate CT between the electron-rich anthracene units and the electron-deficient TNF guest.

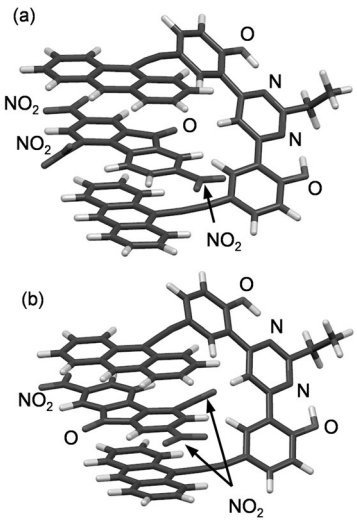

Figure 5. Optimized conformations $Conf_1$ (a) and $Conf_2$ (b) of inclusion complex **1-OH**⊃TNF determined by DFT calculations (B97-D/TZVP).

We attempted to perform ROESY (rotating Overhauser enhancement and exchange spectroscopy) measurements to investigate the actual structure of the inclusion complex, but the poor solubility of TNF prevented this. Therefore, we synthesized a derivative of a TNF isomer with an alkoxycarbonyl substituent at the 2-position of fluorenone (**TNF-C_{16}**). The K_a value of **1-OH** and **TNF-C_{16}** was estimated to be $180\ M^{-1}$, which is lower than that of TNF ($K_a = 2100\ M^{-1}$). The high solubility of **TNF-C_{16}** and the inclusion complex in $CDCl_3$ enabled ROESY measurements. The ^1H NMR and 1D ROESY spectra are shown in Figure 6 ([**1-OH**] = 5.0 mmol L^{-1}, [**TNF-C_{16}**] = 100 mmol L^{-1}). Selective irradiation of H_h ($\delta_H = 8.61$ ppm) in the backbone resulted in a positive peak at $\delta_H = 8.75$ ppm. This suggests an intermolecular correlation between H_h (**1-OH**) and H_B (**TNF-C_{16}**), which indicates intercalation of **TNF-C_{16}** between the two anthryl groups of molecular tweezers **1-OH**. A negative peak at 8.69 ppm can be attributed to the intramolecular correlation (TOCSY) between H_h and H_i of **1-OH**.

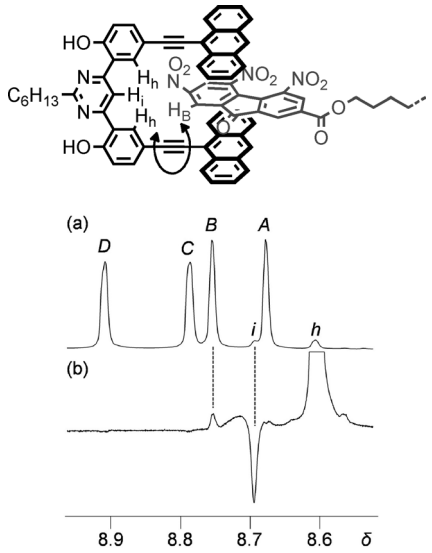

Figure 6. a) ^{1}H NMR and b) 1D ROESY (selective excitation of H_h) spectra of inclusion complex **1-OH**⊃**TNF-C$_{16}$** ($CDCl_3$, [**1-OH**] = 5.0 mmol L^{-1}, [**TNF-C$_{16}$**] = 100 mmol L^{-1}, 298 K, mixing time = 200 ms).

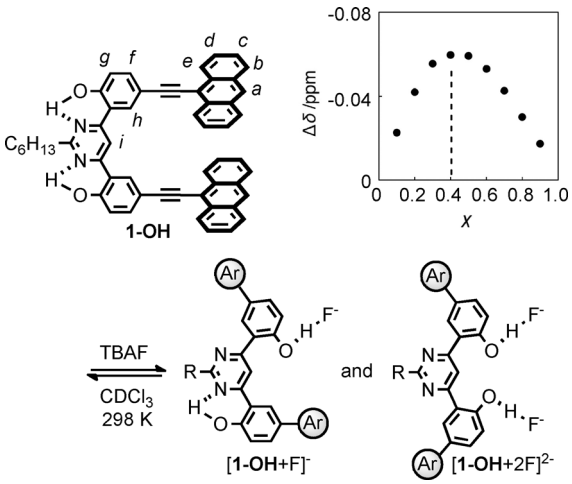

Scheme 4. Deprotonation of molecular tweezers **1-OH** by addition of nBu$_4$NF (TBAF) to form a mixture of 1:1 ([**1-OH** + F]$^-$) and 1:2 ([**1-OH** + 2 F]$^{2-}$) complexes ($CDCl_3$, 298 K). Inset: Job plot of **1-OH** and TBAF determined by ^{1}H NMR titration ($CDCl_3$, [**1-OH**] + [TBAF] = 2.0 mmol L^{-1}, 298 K). R=-C_6H_{13}.

Deprotonation of the host molecule and complex

Figure 7 shows the results of ^{1}H NMR titration of molecular tweezers **1-OH** with tetra-*n*-butylammonium fluoride (TBAF) in $CDCl_3$ at 298 K ([**1-OH**] = 1.0 mmol L^{-1}, [TBAF] = 0.05–10.0 mmol L^{-1}). The addition of TBAF to a solution of **1-OH** in $CDCl_3$ caused a significant shift and broadening of aromatic hydrogen peaks (H_f, H_g, H_h, H_i) of the backbone. Comparison of Figure 7 i and x suggests that the peak due to H_h is shifted by 0.20 ppm to lower field on complexation of F$^-$. The peaks of H_f and H_g also show large shifts (0.18 and 0.20 ppm, respectively), suggesting significant change of the electronic state of the aromatic rings. Scheme 4 depicts a plausible structural change of the molecule caused by addition of F$^-$. Addition of fluoride to **1-OH** cleaves an OH···N hydrogen bond. Facile rotation about the C–C bond between pyrimidine and phenol rings changes the conformation of the molecule, so that the bulky anthryl rings are orientated in less sterically crowded directions in an S-type structure (Scheme 4, [**1-OH** + F]$^-$). The addition of two fluoride ions cleaves both of the OH···N hydrogen bonds of **1-OH**. The resulting dianionic species prefers to form a W-shaped structure by rotation about the two C–C bonds, similar to the *O*-alkylated molecular tweezers.[18]

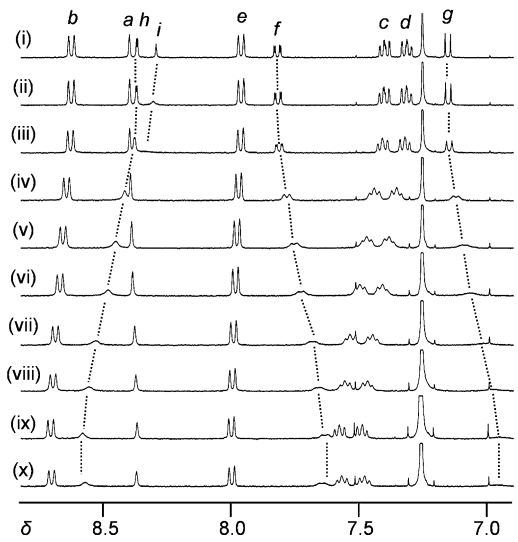

Figure 7. ^{1}H NMR titration of **1-OH** with TBAF (400 MHz, $CDCl_3$, 298 K, [**1-OH**] = 1.0 mmol L^{-1}). i) [TBAF] = 0.0, ii) 0.05, iii) 0.10, iv) 0.50, v) 1.0, vi) 2.0, vii) 3.0, viii) 5.0, ix) 8.0, and x) 10.0 mmol L^{-1}. The dotted lines indicate shifts of the signals of the backbone protons of molecular tweezers (**1-OH**).

The Job plot of **1-OH** and TBAF, monitored by ^{1}H NMR titration in $CDCl_3$ at 298 K ([**1-OH**] + [TBAF] = 2.0 mmol L^{-1}), shows a maximum at X = 0.40 (Scheme 4 inset). The result is ascribed to formation of both 1:1 (X = 0.50) and 1:2 (X = 0.33) complexes of **1-OH** and TBAF, accompanied by cleavage of one and two OH···N hydrogen bonds of **1-OH**, respectively.[23] The K_a value for fluoride addition was estimated to be 820 M^{-1} by means of a Scatchard plot in $CDCl_3$ at 298 K.

Addition of TBAF to inclusion complex **1-OH**⊃TNF also caused cleavage of the OH···N hydrogen bonds and release of TNF owing to a change in molecular conformation of **1-OH**. The results of the ^{1}H NMR titration ($CDCl_3$, [**1-OH**] = 1.0 mmol L^{-1}, [TNF] = 1.0 mmol L^{-1}, [TBAF] = 0–10 mmol L^{-1}, 298 K) are shown in Figure 8. Increasing the amount of added TBAF changed the peak positions of TNF and anthryl groups. The peaks due to phenoxyl groups (H_f and H_g) showed similar changes on titration of **1-OH** with TBAF (Figure 7), although the shift of H_h is much less significant. The spectrum after addition of 20.0 equivalents of TBAF to the $CDCl_3$ solution (Figure 8 vii) contains signals at similar positions to the deprotonated molecular tweezers (Figure 7 x). These results indicate that addition of TBAF to inclusion complex **1-OH**⊃TNF causes decomplexation of the inclusion complex to form the deprotonated molecular tweezers and free TNF (Scheme 5). Addition of an excess of Lewis acid (BF_3·OEt_2, ca. 100 mmol L^{-1}) regenerates

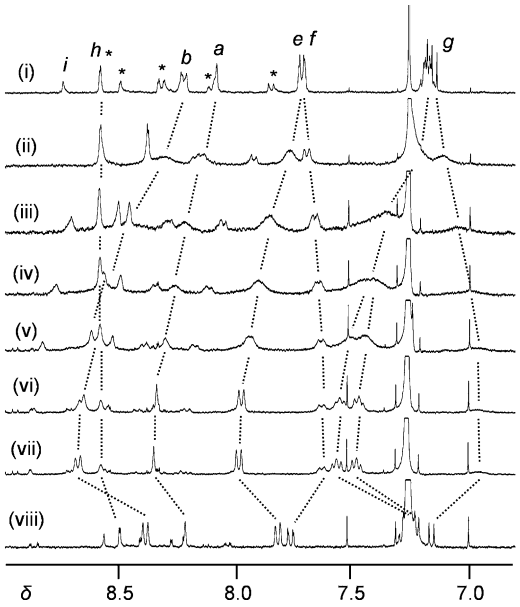

Figure 8. ^{1}H NMR titration of **1-OH**⊃TNF with TBAF (400 MHz, $CDCl_3$, 298 K, [**1-OH**] = 1.0 mmol L^{-1}, [TNF] = 1.0 mmol L^{-1}). i) [TBAF] = 0.0, ii) 1.0, iii) 2.0, iv) 3.0, v) 5.0, vi) 8.0, vii) 10.0 mmol L^{-1}, viii) + BF_3·OEt_2 (excess). The dotted lines indicate shifts of the signals of molecular tweezers **1-OH**. The asterisks denote signals of TNF.

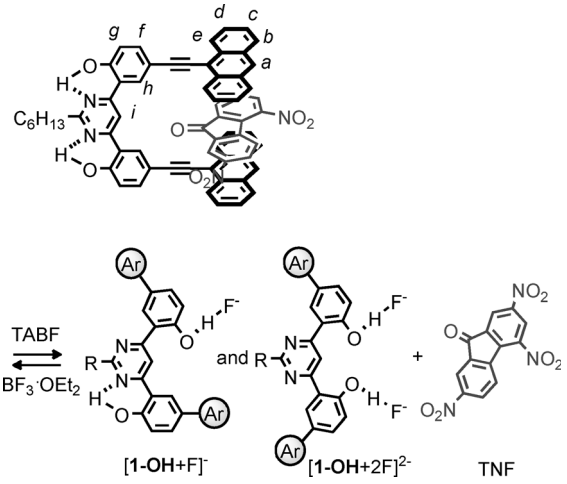

Scheme 5. Decomplexation of the inclusion complex **1-OH**⊃TNF by addition of TBAF ($CDCl_3$, 298 K). R=-C_6H_{13}.

1-OH (Figure 8 viii). The signals due to **1-OH** (H_a–H_g) of the mixture are observed at lower field than in the original spectrum (Figure 8 i), but much closer than in the mixture before addition of BF_3 (Figure 8 vii). The peaks of TNF included in the complex are also clearly observed at δ_H = 8.88, 8.42, 8.28, 8.23, and 8.04 ppm, at positions close to those in Figure 8 i.

Deprotonation of a model compound of **1-OH**, namely, 4-(2-hydroxyphenyl)-2-methylpyrimidine (**7-OH**), by F^- was investigated by DFT calculations [PCM-B97-1/DZV + (d,p)] in $CHCl_3$. The free energy of formation of [**7-OH** + F]$^-$ from **7-OH** and F^- was calculated to have a large negative value (ΔG = −18.3 kJ mol^{-1}; Figure 9). The formation of the stable OH···F hydrogen bond may compensate for rotation about the C–C

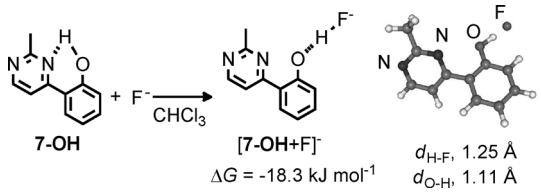

Figure 9. Free-energy change ΔG for deprotonation of model compound **7-OH** from DFT calculations [PCM-B97-1/DZV + (d,p)]. nBu_4N^+ was ignored in the calculation because of F^- of TBAF is regarded as a naked anion in $CHCl_3$.

bond between the pyrimidine and bulky substituent. Concurrent of addition of two fluoride ions to **1-OH** is ascribed to the large energy difference between the intramolecular OH···N hydrogen bonds and intermolecular O···HF hydrogen bonds.

Photochemical properties

UV/Vis and fluorescence spectra of molecular tweezers **2-OH** and **3-OH**, their *O*-alkylated derivatives **2-OHex** and **3-OHex**, and model compound 9-(4-hydroxyphenyl)anthracene (**8-OH**) are shown in Figure 10. The absorption and fluorescence data are summarized in Table 2.

These compounds show typical absorption bands due to the π–π* transition of the anthryl group at similar positions (λ_{max} = 368–405 nm) and at longer wavelength than anthracene

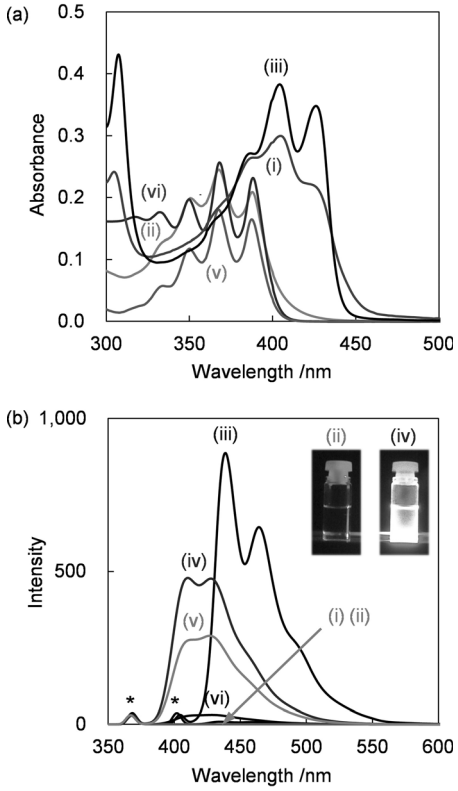

Figure 10. a) UV/Vis ($CHCl_3$, [compound] = 0.010 mmol L^{-1}, RT) and b) fluorescence spectra ($CHCl_3$, [compound] = 0.0010 mmol L^{-1}, RT) of i) **2-OH**, ii) **3-OH**, iii) **2-OHex**, iv) **3-OHex**, v) **8-OH**, and vi) **8-OH** + pyridine ([pyridine] = 100 mmol L^{-1}). The asterisks in b) indicate the excitation light. The insets show the fluorescence of ii) **3-OH** and iv) **3-OHex** in $CHCl_3$ under UV irradiation (365 nm).

Table 2. Absorption and fluorescence data.

Compound	Absorption		Fluorescence[c]	
	λ_{max} [nm]	ε [$M^{-1}cm^{-1}$]	λ_{max} [nm]	ϕ[a]
2-OH	405	30000	–	<0.01
3-OH	368	24500	–	<0.01
2-OHex	404	38300	439	0.40
3-OHex	368	25700	410, 428	0.39
8-OH	368	9700	412, 429	0.33 (0.36[b])
anthracene	359	7200	405	0.09[b]

[a] Standard sample: quinine (in 0.5 mmol L^{-1} H_2SO_4 aq., $\phi=0.546$). [b] Determined at 0.0020 mmol L^{-1} in $CHCl_3$. [c] $\lambda_{ex}=\lambda_{max}$(abs).

($\lambda_{max}=359$ nm). The absorption bands of **3-OH** trail up to about 440 nm, and its $CHCl_3$ solutions show a yellow color, whereas solutions of **3-OHex** are colorless, which is attributed to a intramolecular CT excitation between electron-rich anthryl groups and the electron-deficient backbone unit. Three aromatic rings of the backbone structure of **3-OH** are aligned in a planar fashion owing to the intramolecular OH···N hydrogen bonds and form an electron-poor π surface, which induces a decrease in the LUMO level, so that **3-OH** can absorb longer wavelengths than **3-OHex** due to the intramolecular CT excitation.

Excitation of **2-OHex** and **3-OHex** at 404, 368 nm (in $CHCl_3$) induces a strong fluorescence at 439, 410 nm, which corresponds to π–π^* transition of the anthryl groups. The quantum yields of **2-OHex** ($\phi=0.40$) and **3-OHex** ($\phi=0.39$) are higher than that of anthracene ($\phi=0.09$). The fluorescence of **2-OH** and **3-OH** under the same conditions is almost negligible ($\phi<0.01$) despite the presence of anthracene rings. Model compound **8-OH** can be regarded as a partial structure of molecular tweezers **3-OH**, but **8-OH** showed strong fluorescence ($\phi=0.33$). The addition of an excess of pyridine to a solution of **8-OH** in $CHCl_3$ ([**8-OH**] = 0.0010 mmol L^{-1}, [pyridine] = 100 mmol L^{-1}) decreased the fluorescence intensity to $\phi=0.05$.

The efficient quenching of fluorescence of **8-OH** in the presence of pyridine is ascribed to an intermolecular photoinduced electron-transfer (PET) process.[24] The electron-rich phenoxyl group undergoes partial deprotonation with pyridine and transfers an electron to an excited state of the anthryl group (Figure 11 a). Much weaker fluorescence of molecular tweezers **2-OH** and **3-OH** compared to *O*-alkylated compounds **2-OHex** and **3-OHex** is also explained by the PET process. The phenoxyl groups are formed by OH···N hydrogen bonds with the neighboring pyrimidinyl groups (Figure 11 b).

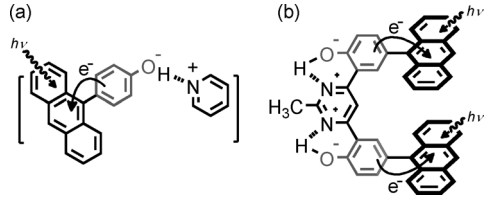

Figure 11. Plausible quenching mechanism of a) **8-OH** + pyridine and b) **3-OH** by PET processes.

Conclusion

We have synthesized molecular tweezers with anthrylethynyl arms and a 4,6-bis(2-hydroxyaryl)pyrimidine backbone spacer. Their U-shaped conformation is stabilized by intramolecular OH···N hydrogen bonds between the pyrimidinyl nitrogen atoms and the OH groups. Formation of host–guest complexes was confirmed by ^{1}H NMR and UV/Vis spectroscopy as well as by theoretical studies. **1-OH** and TNF formed a 1:1 host–guest complex in $CDCl_3$, the association constant K_a of which was estimated to be 2100 M^{-1}, which is larger than those of known molecular tweezers ($K_a<1000$ M^{-1}). This is ascribed to the intramolecular hydrogen bonds formed by the backbone unit. The U-shaped conformation of **1-OH** can be switched to W- and S-shaped structures by the addition of F^- with cleavage of the OH···N hydrogen bonds. Thus, we demonstrated decomplexation of host–guest complex **1-OH**⊃TNF by fluoride-induced transformation of **1-OH** into an unfavorable conformation for guest binding.

Experimental Section

The synthesis of molecular tweezers **1-OH**, **2-OH**, and **2-OHex** is summarized in Scheme 6. 9-Ethynylanthracene,[25] 4,6-diiodo-2-chloropyrimidine,[26] and 4,5,7-trinitro-9-fluorenone-2-carboxylic acid[27] were prepared by literature methods. Syntheses of **6-OH**, **6-OMe**, **3-OH**, **3-OHex**, **8-OH** were previously reported.[18] Anhydrous solvents were purchased and used without further purification. Other materials were commercially available and used without further purification. ^{1}H and $^{13}C\{^1H\}$ NMR spectra were acquired on a Bruker AV-400M spectrometer (400 MHz). The chemical sifts were referenced to TMS ($\delta=0.00$) for ^{1}H and $CDCl_3$ ($\delta=77.16$), $C_2D_2Cl_4$ ($\delta=74.20$) for ^{13}C as internal standards. Fast atom bombardment mass spectra (FAB MS) were measured on a JEOL JMS-700 (3-nitrobenzyl alcohol (NBA) matrix). High-resolution ESI MS spectra were measured with a Bruker micrOTOF II (eluent: acetone + 1 %CF_3COONa). Elemental analyses were obtained from a Yanaco MT-5 CHN autorecorder. IR absorption spectra were measured on Shimadzu FTIR-8100 and a JASCO FTIR-4100 spectrometers. UV/Vis absorption spectra were measured on a JASCO V-530 spectrometer. Emission spectra were measured on a JASCO FP-6300 spectrometer. X-ray crystal structure analyses were performed at a Rigaku AFC-10R Saturn CCD diffractometer or a Bruker APEXII ULTRA/CCD diffractometer with graphite-monochromated $Mo_{K\alpha}$ radiation.

4,6-Bis(5-bromo-2-methoxyphenyl)-2-chloropyrimidine (4-OMe)

A mixture of 4,6-diiodo-2-chloropyrimidine (1.83 g, 5.0 mmol), 5-bromo-2-methoxyphenylboronic acid (2.31 g, 10 mmol), K_2CO_3 (2.76 g, 20 mmol), and [$Pd(PPh_3)_4$] (353 mg, 0.31 mmol) was dissolved in 1,4-dioxane (75 mL)/H_2O (25 mL) under argon atmosphere. After stirring for 24 h at 80 °C, the mixture was allowed to cool to room temperature. The solid that separated from the solution was removed by filtration, and the filtrate was evaporated to dryness. The obtained yellow oil was dissolved in CH_2Cl_2 (300 mL) and the solution was washed with water (2×100 mL). The separated organic phase was dried over $MgSO_4$, filtered, and evaporated to give the crude product as a yellow oil, which was purified by column chromatography on silica gel (eluent: CH_2Cl_2/hexane 10/3)

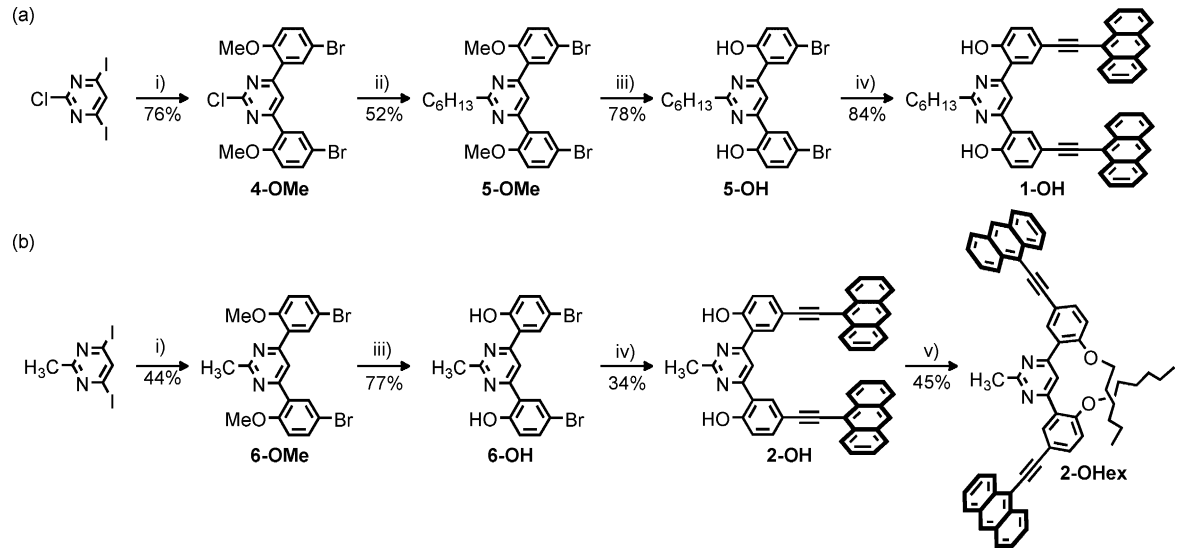

Scheme 6. Synthesis of molecular tweezers. a) **1-OH**, b) **2-OH**, and c) **2-OHex**. i) 5-Bromo-2-methoxyphenylboronic acid, $[Pd(PPh_3)_4]$, K_2CO_3, 1,4-dioxane, H_2O, 80 °C, 18–24 h; ii) $C_6H_{13}MgBr$, $Fe(acac)_3$, THF, *N*-methylpyrrolidone, RT, 1 h; iii) BBr_3, CH_2Cl_2, RT to reflux, 17–22 h; iv) 9-Ethynylanthracene, $Pd(OAc)_2$, PPh_3, CuI, iPr_2NH, THF, 70 °C, 24 h; v) $C_6H_{13}I$, K_2CO_3, $CH_3COC_2H_5$, 80 °C, 19 h.

to yield **4-OMe** (1.83 g, 3.8 mmol, 76%) as a white solid. ^{1}H NMR (400 MHz, $CDCl_3$, RT): $\delta = 8.48$ (s, 1H, C_4N_2H), 8.17 (d, 2H, C_6H_3, $J =$ 2.8 Hz), 7.56 (dd, 2H, C_6H_3, $J = 2.4$, 8.8 Hz), 6.92 (d, 2H, C_6H_3, $J =$ 8.8 Hz), 3.91 ppm (s, 6H, Me); ^{13}C NMR (100 MHz, $CDCl_3$, RT): $\delta =$ 164.1, 160.9, 157.3, 134.9, 134.2, 127.0, 120.6, 113.8, 113.6, 56.1 ppm; FAB MS (NBA matrix) calcd for $C_{18}H_{13}Br_2ClN_2O_2$: 484; found: *m/z* 485 $[M+H^+]$; elemental analysis calcd (%) for $C_{18}H_{13}Br_2ClN_2O_2$: C 44.62, H 2.70, N 5.78; found: C 44.55, H 2.67, N 5.77.

4,6-Bis(5-bromo-2-methoxyphenyl)-2-hexylpyrimidine (5-OMe)

A mixture of **4-OMe** (1.70 g, 3.5 mmol) and $Fe(acac)_3$ (37 mg, 0.11 mmol) was dissolved in dry THF (30 mL) and *N*-methylpyrrolidone (3.0 mL). $C_6H_{13}MgBr$ (3.9 mmol, 3.9 mL of a 1.0 M solution in THF) was added dropwise to the solution under argon at 0 °C. The mixture was stirred at room temperature for 1 h. The reaction mixture was quenched by addition of water (1 mL) followed by evaporation of the solvent. The obtained brown oil was dissolved in CH_2Cl_2 (300 mL) and washed with water (100 mL) and brine (100 mL). The separated organic phase was dried over $MgSO_4$, filtered, and evaporated to give a crude product, which was purified by column chromatography on silica gel (eluent: CH_2Cl_2/hexane 10/3) to obtain **5-OMe** (969 mg, 1.8 mmol, 52%) as a white solid. ^{1}H NMR (400 MHz, $CDCl_3$, RT): $\delta = 8.17$ (s, 1H, C_4N_2H), 8.09 (d, 2H, C_6H_3, $J = 2.4$ Hz), 7.51 (dd, 2H, C_6H_3, $J = 2.8$, 8.8 Hz), 6.90 (d, 2H, C_6H_3, $J = 8.8$ Hz), 3.88 (s, 6H, OCH_3), 3.05 (t, 2H, CH_2, $J = 7.6$ Hz), 1.92 (m, 2H, CH_2), 1.49–1.34 (m, 6H, CH_2), 0.93 ppm (t, 3H, CH_3, $J =$ 6.9 Hz); ^{13}C NMR (100 MHz, $CDCl_3$, RT): $\delta = 171.5$, 161.3, 157.0, 133.9, 133.8, 129.3, 119.5, 113.8, 113.5, 56.1, 40.0, 31.9, 29.4, 29.1, 22.8, 14.3 ppm; FAB MS (NBA matrix) calcd for $C_{24}H_{26}Br_2N_2O_2$: 534; found: *m/z* 535 $[M+H^+]$.

4,6-Bis(5-bromo-2-hydroxyphenyl)-2-hexylpyrimidine (5-OH)

BBr_3 (20 mmol, 20 mL of a 1.0 M solution in CH_2Cl_2) was slowly added to a solution of **4-OMe** (1.05 g, 2.0 mmol) in CH_2Cl_2 (60 mL) at 0 °C. The mixture was stirred at room temperature for 4 h then heated at reflux for 16 h. The resulting mixture was cooled to 0 °C and the reaction was quenched by addition of cold water (100 mL) and CH_2Cl_2 (200 mL). The separated organic phase was washed with water (100 mL), dried over $MgSO_4$, and evaporated to yield a yellow solid. The crude product was purified by reprecipitation from CH_2Cl_2 (30 mL)/methanol (150 mL) to yield **5-OH** (784 mg, 1.5 mmol, 78%) as a yellow solid. ^{1}H NMR (400 MHz, $CDCl_3$, RT): $\delta =$ 13.78 (s, 2H, OH), 8.03 (d, 2H, C_6H_3, $J = 2.4$ Hz), 7.96 (s, 1H, C_4N_2H), 7.51 (dd, 2H, C_6H_3, $J = 2.4$, 8.8 Hz), 6.97 (d, 2H, C_6H_3, $J = 8.8$ Hz), 3.06 (t, 2H, CH_2, $J = 7.6$ Hz), 1.91 (tt, 2H, CH_2, $J = 7.2$, 14.8 Hz), 1.44–1.32 (m, 6H, CH_2), 0.90 ppm (t, 3H, CH_3, $J = 7.2$ Hz); $^{13}C\{^1H\}$ NMR (100 MHz, $CDCl_3$, RT): $\delta = 167.6$, 164.3, 160.5, 136.8, 129.5, 121.3, 118.5, 111.4, 106.2, 38.7, 31.6, 29.0, 27.8, 22.6, 14.2 ppm; FAB MS (NBA matrix) calcd for $C_{22}H_{22}Br_2N_2O_2$: 506; found: *m/z* 507 $[M+H^+]$; elemental analysis calcd (%) for $C_{22}H_{22}Br_2N_2O_2$: C 52.20, H 4.38, N 5.53; found: C 52.10, H 4.15, N 5.50.

4,6-Bis[5-(anthracen-9-ylethynyl)-2-hydroxyphenyl]-2-hexylpyrimidine (1-OH)

A mixture of **5-OH** (244 mg, 0.48 mmol), PPh_3 (15.6 mg, 0.059 mmol), $Pd(OAc)_2$ (4.5 mg, 0.020 mmol), CuI (4.2 mg, 0.022 mmol), and 9-ethynylanthracene (403 mg, 1.99 mmol) was dissolved in iPr_2NH (10 mL)/THF (10 mL) under argon. After the mixture was stirred at 70 °C for 24 h, the solids that separated from the solution were removed by filtration followed by evaporation of the filtrate. The obtained yellow oil was dissolved in CH_2Cl_2 (200 mL) and the solution was washed with 10% HCl aq. (50 mL) and water (2×50 mL). The separated organic phase was dried over $MgSO_4$, filtered, and evaporated to form a crude product, which was purified by column chromatography on silica gel (eluent: CH_2Cl_2/hexane 10/3) and reprecipitation (CH_2Cl_2/CH_3CN 10/100 mL) to yield **1-OH** (302 mg, 0.40 mmol, 84%) as an orange solid. ^{1}H NMR (400 MHz, $CDCl_3$, RT): $\delta = 14.19$ (br, 2H, OH), 8.62 (d, 4H, $C_{14}H_9$, $J = 8.6$ Hz), 8.38 (s, 2H, $C_{14}H_9$), 8.33 (d, 2H, C_6H_3, $J = 2.0$ Hz), 8.22 (s, 1H, C_4N_2H), 7.95 (d, 4H, $C_{14}H_9$, $J = 8.4$ Hz), 7.80 (dd, 2H, C_6H_3, $J = 1.9$, 8.5 Hz), 7.40 (ddd, 4H, $C_{14}H_9$, $J = 1.1$, 6.6, 7.8 Hz), 7.31 (ddd, 4H, $C_{14}H_9$, $J = 0.8$, 6.6, 7.7 Hz), 7.14 (d, 2H, C_6H_3, $J = 8.5$ Hz), 3.08 (t, 2H, CH_2, $J = 7.7$ Hz), 1.96 (tt, 2H, CH_2, $J = 7.8$, 15.0 Hz), 1.50 (tt, 2H, CH_2, $J = 7.8$, 14.6 Hz), 1.39 (m, 4H, CH_2), 0.93 ppm (t, 3H, CH_3, $J = 7.1$ Hz); $^{13}C\{^1H\}$ NMR (100 MHz, $CDCl_3$, RT): $\delta = 166.9$, 164.3,

161.8, 137.1, 132.6, 131.2, 130.7, 128.7, 127.6, 126.8, 126.7, 125.8, 119.7, 117.3, 117.1, 114.8, 106.0, 100.2 (C≡C), 85.4 (C≡C), 38.5, 31.7, 29.1, 27.6, 22.7, 14.2 ppm; IR (KBr disk, RT): $\tilde{\nu}$ = 3050, 2952, 2925, 2854, 2592 (O–H···N), 2197 (C≡C), 1608, 1574, 1537, 1482, 1467, 1418, 1406, 1291, 879, 855, 839, 826, 784, 734, 678, 663, 614, 551, 512 cm^{-1}; FAB MS (NBA matrix) calcd for $C_{54}H_{40}N_2O_2$: 748, found: *m/z* 749 [*M*+H$^+$]; elemental analysis calcd (%) for $C_{54}H_{40}N_2O_2$ 86.60, H 5.38, N 3.74; found: C 86.40, H 4.97, N 3.62.

4,6-Bis[5-(anthracen-9-ylethynyl)-2-hydroxyphenyl]-2-methylpyrimidine (2-OH)

A mixture of **6-OH** (87 mg, 0.20 mmol), PPh_3 (32 mg, 0.12 mmol), $Pd(OAc)_2$ (9.0 mg, 0.040 mmol), CuI (7.6 mg, 0.040 mmol), and 9-ethynylanthracene (121 mg, 0.60 mmol) was dissolved in *i*Pr_2NH (3 mL)/THF (1 mL) under argon. After the mixture was stirred at 70 °C for 24 h, the undissolved solids were removed by filtration followed by evaporation of the filtrate. The obtained orange solid was dissolved in CH_2Cl_2 (150 mL) and the solution was washed with 10% HCl aq. (50 mL) and water (2×50 mL). The separated organic phase was dried over $MgSO_4$, filtered, and evaporated to give a crude product, which was purified by column chromatography on silica gel (eluent: $CHCl_3$) to yield **2-OH** (52 mg, 0.076 mmol, 38%) as an orange solid. ^{1}H NMR (400 MHz, $CDCl_3$, RT): δ = 13.80 (br, 2H, OH), 8.63 (d, 4H, $C_{14}H_9$, *J* = 8.8 Hz), 8.41 (s, 2H, $C_{14}H_9$), 8.38 (d, 2H, C_6H_3, *J* = 2.0 Hz), 8.32 (s, 1H, C_4N_2H), 7.97 (d, 4H, $C_{14}H_9$, *J* = 8.4 Hz), 7.83 (dd, 2H, C_6H_3, *J* = 2.0, 8.4 Hz), 7.40 (ddd, 4H, $C_{14}H_9$, *J* = 1.2, 6.5, 7.8 Hz), 7.32 (ddd, 4H, $C_{14}H_9$, *J* = 1.0, 6.6, 7.8 Hz), 7.16 (d, 2H, C_6H_3, *J* = 8.4 Hz), 2.87 ppm (s, 3H, CH_3); ^{13}C{^{1}H} NMR (100 MHz, $C_2D_2Cl_4$, RT): δ = 164.7, 163.9, 161.8, 137.5, 132.7, 131.3, 130.9, 128.9, 128.0, 127.2, 126.8, 126.1, 120.0, 117.3, 117.2, 115.0, 106.5, 100.4 (C≡C), 85.7 (C≡C), 25.7 ppm; IR (KBr disk, RT): $\tilde{\nu}$ = 3050, 3020, 2550 (O–H···N), 2251 (C≡C), 1577, 1537, 1438, 1418, 1288, 1263, 1221, 1185, 1131, 882, 852, 824, 749, 732, 660, 614, 549, 510 cm^{-1}; FAB MS (NBA matrix) calcd for $C_{49}H_{30}N_2O_2$: 678; found: *m/z* 679 [*M*+H$^+$]; elemental analysis calcd (%) for $C_{49}H_{30}N_2O_2$ + 1.2 $CHCl_3$: C 73.35, H 3.83, N 3.41; found: C 73.05, H 3.92, N 3.48.

4,6-Bis{5-(anthracen-9-ylethynyl)-2-(hexyloxy)phenyl}-2-methylpyrimidine (2-OHex)

2-OH (203 mg, 0.30 mmol), K_2CO_3 (248 mg, 1.8 mmol), and $C_6H_{13}I$ (180 μL, 1.2 mmol) were dissolved in $CH_3COC_2H_5$ (15 mL). After the mixture was stirred at 80 °C for 19 h, the solids were removed by filtration followed by evaporation of the filtrate. The obtained solid was dissolved in CH_2Cl_2 (50 mL) and the solution was washed with water (2×20 mL). The separated organic phase was dried over $MgSO_4$, filtered, and evaporated to give a crude product, which was purified by column chromatography on silica gel (eluent: CH_2Cl_2) to yield **2-OHex** (114 mg, 0.13 mmol, 45%) as yellow powder. ^{1}H NMR (400 MHz, $CDCl_3$, RT): δ = 8.69 (d, 4H, $C_{14}H_9$, *J* = 8.7 Hz), 8.41 (s, 2H, $C_{14}H_9$), 8.34 (d, 2H, C_6H_3, *J* = 2.1 Hz), 8.33 (s, 1H, C_4N_2H), 8.02 (d, 4H, $C_{14}H_9$, *J* = 8.4 Hz), 7.81 (dd, 2H, C_6H_3, *J* = 2.2, 8.4 Hz), 7.60 (ddd, 4H, $C_{14}H_9$, *J* = 1.1, 6.5, 7.8 Hz), 7.51 (ddd, 4H, $C_{14}H_9$, *J* = 0.9, 6.6, 8.1 Hz), 7.07 (d, 2H, C_6H_3, *J* = 8.6 Hz), 4.10 (t, 4H, OCH_2, *J* = 6.3 Hz), 2.96 (s, 3H, CH_3), 1.76 (m, 4H, CH_2), 1.38 (m, 4H, CH_2), 1.23–1.09 (m, 8H, CH_2), 0.77 ppm (t, 6H, *J* = 7.0 Hz); ^{13}C{^{1}H} NMR (100 MHz, $CDCl_3$, RT): δ = 168.1, 162.3, 157.6, 136.4, 134.5, 132.7, 131.4, 128.8, 128.1, 127.5, 127.1, 126.6, 125.8, 119.9, 117.8, 116.5, 112.9, 100.7 (C≡C), 85.6 (C≡C), 69.1, 31.7, 29.3, 26.7, 26.1, 22.6, 14.1 ppm; IR (KBr disk, RT): $\tilde{\nu}$ = 3046, 2925, 2855, 2204 (C≡C), 1605, 1574, 1530, 1496, 1465, 1439, 1389, 1334, 1263, 1251, 1146, 1044, 877, 842, 813, 783, 729, 615, 550, 408 cm^{-1}; FAB MS (NBA matrix) calcd for $C_{61}H_{54}N_2O_2$: 846; found: *m/z* 847 [*M*+H$^+$]; elemental analysis calcd (%) for $C_{61}H_{54}N_2O_2$ + H_2O: C 84.69, H 6.52, N 3.24; found: C 84.96, H 6.40, N 3.10. (Scheme 6)

4,5,7-Trinitro-9-fluorenone-2-carboxylic acid[27]

9-Fluorenone-2-carboxylic acid (2.26 g, 10 mmol) was slowly added a solution of fuming HNO_3 (40 mL) and conc. H_2SO_4 (40 mL) at 0 °C and the mixture was heated to reflux for 3 h. After cooling to RT, the yellow solution was poured into 400 mL of crushed ice. The resulting yellow precipitate was collected by suction filtration. The crude product was purified by reprecipitation from CH_3NO_2/CH_2Cl_2 to yield 4,5,7-trinitro-9-fluorenone-2-carboxylic acid (2.87 g, 8.0 mmol, 79%) as a pale yellow solid. ^{1}H NMR is matched with the reported literature.[27]

Hexadecyl 4,5,7-trinitro-9-fluorenone-2-carboxylate (TNF-C_{16})

A mixture of 4,5,7-trinitro-9-fluorene-2-carboxylic acid (1.06 g, 2.9 mmol), 1-ethyl-3-(3-dimethylaminopropyl) carbodiimide hydrochloride (0.675 g, 3.5 mmol), 4-dimethylaminopyridine (0.042 g, 0.34 mmol), and cetyl alcohol (0.741 g, 3.1 mmol) was dissolved in CH_2Cl_2 (100 mL) under argon. After the mixture was stirred at RT for 14 h, the solution was washed with 10% HCl aq. (100 mL), water (100 mL) and brine (100 mL). The separated organic phase was dried over $MgSO_4$, filtered, and evaporated to give a crude product, which was purified by column chromatography on silica gel (eluent: CH_2Cl_2/hexane 2/1) to yield **TNF-C_{16}** (1.09 g, 1.9 mmol, 63%) as a pale yellow solid. ^{1}H NMR ($CDCl_3$, RT): δ = 8.99 (d, 1H, $C_{13}H_4O$, *J* = 2.0 Hz), 8.85 (d, 1H, $C_{13}H_4O$, *J* = 2.1 Hz), 8.81 (d, 1H, $C_{13}H_4O$, *J* = 1.5 Hz), 8.72 (d, 1H, $C_{13}H_4O$, *J* = 1.5 Hz), 4.44 (t, 2H, OCH_2, *J* = 6.8 Hz), 1.83 (tt, 2H, CH_2, *J* = 7.0, 13.8 Hz), 1.94–1.20 (m, 26H, CH_2), 0.88 ppm (t, 3H, CH_3, *J* = 6.6 Hz); ^{13}C{^{1}H} NMR ($CDCl_3$, RT): δ = 185.1, 162.8, 149.7, 146.9, 146.6, 138.6, 138.5, 137.8, 136.2, 136.1, 131.7, 129.3, 125.5, 122.7, 67.2, 32.0, 29.8, 29.8–29.7, 29.6 29.5, 29.4, 28.7, 26.0, 22.8, 14.2 ppm; ESI TOF MS (eluent: acetone + 1% CF_3COONa) calcd for $C_{30}H_{37}N_3O_9$ + Na^+: 606.2422; found: *m/z* 606.2431 [*M*+Na]$^+$.

Computational methods

The relative free energies of $Conf_1$ and $Conf_2$ were obtained by using the empirical dispersion-corrected B97-D density functional and TZVP basis set with density fitting approximations and TZVPFit auxiliary basis set. The calculations were performed with the Gaussian 09 program package.[28] The free-energy change of the reaction between **7-OH** and fluoride anion was calculated with the B97-1 density functional and DZV + (d,p) basis set. The effect of solvation was considered by using the conductor-like polarizable continuum model (PCM) with the parameters of $CHCl_3$. The calculation was performed with GAMESS 2013 (R1).[29] These free energies were obtained as a total electronic energies and an unscaled Gibbs free-energy correction. All structures were optimized and verified to be local minima by Hessian calculation.

X-ray diffraction

Single crystals suitable for X-ray diffraction studies were obtained by recrystallization from $CHCl_3$ (**2-OH**) and CH_2Cl_2/hexane (**2-OHex**). Crystallographic data and detailed results of refinement are summarized in Table S1 of the Supporting Information. CCDC 937957 (**2-OH**), 937958 (**2-Ohex**), 822408 (**3-OH**·2 $CHCl_3$) and 822409 (**3-OHex**) contain the supplementary crystallographic data for this paper. These data can be obtained free of charge from The Cam-

bridge Crystallographic Data Centre via www.ccdc.cam.ac.uk/data_request/cif.

Acknowledgements

This research was supported by Global COE program and KAKENHI from the Japan Society for the Program of Science (JSPS). Y.T. thanks JSPS Research fellowship for Young Scientists. This work was supported by a Grant-in-Aid for Scientific Research on Innovative Areas "The Coordination Programming (24108711)". We thank our colleagues in the Center for Advanced Materials Analysis, Technical Department, Tokyo Institute of Technology for NMR and X-ray analysis as well as MS measurement.

Keywords: host–guest systems · hydrogen bonds · molecular tweezers · pi interactions · supramolecular chemistry

[1] a) C. J. Pedersen, *J. Am. Chem. Soc.* **1967**, *89*, 7017 – 7036; b) J. Szejtli, *Chem. Rev.* **1998**, *98*, 1743 – 1753; c) A. Ikeda, S. Shinkai, *Chem. Rev.* **1997**, *97*, 1713 – 1734.

[2] C. W. Chen, H. W. Whitlock, Jr., *J. Am. Chem. Soc.* **1978**, *100*, 4921 – 4922.

[3] a) J. Leblond, A. Petitjean, *ChemPhysChem* **2011**, *12*, 1043 – 1051; b) M. Hardouin-Lerouge, P. Hudhomme, M. Sallé, *Chem. Soc. Rev.* **2011**, *40*, 30 – 43.

[4] a) S. C. Zimmerman, C. M. VanZyl, *J. Am. Chem. Soc.* **1987**, *109*, 7894 – 7896; b) S. C. Zimmerman, C. M. VanZyl, G. S. Hamilton, *J. Am. Chem. Soc.* **1989**, *111*, 1373 – 1381; c) S. C. Zimmerman, Z. Zeng, W. Wu, D. E. Reichert, *J. Am. Chem. Soc.* **1991**, *113*, 183 – 196; d) S. C. Zimmerman, K. W. Saionz, Z. Zeng, *Proc. Natl. Acad. Sci. USA* **1993**, *90*, 1190 – 1193; e) S. C. Zimmerman, K. W. Saionz, *J. Am. Chem. Soc.* **1995**, *117*, 1175 – 1176; f) S. C. Zimmerman, *Top. Curr. Chem.* **1993**, *165*, 71 – 102.

[5] a) S. H. Lee, K. Imamura, J. Otsuki, K. Araki, M. Seno, *J. Chem. Soc. Perkin Trans. 2* **1996**, 847 – 852; b) J. Otsuki, H. Matsui, K. Imamura, I. Yoshikawa, K. Araki, M. Seno, *Chem. Lett.* **2001**, *30*, 1144 – 1145; c) Y. Hisamatsu, H. Aihara, *Chem. Commun.* **2010**, *46*, 4902 – 4904; d) T. Haino, T. Fujii, Y. Fukazawa, *J. Org. Chem.* **2006**, *71*, 2572 – 2580; e) B. Legouin, P. Uriac, S. Tomasi, L. Toupet, A. Bondon, P. van de Weghe, *Org. Lett.* **2009**, *11*, 745 – 748; f) M. Skibiński, R. Gómez, E. Lork, V. A. Azov, *Tetrahedron* **2009**, *65*, 10348 – 10354; g) C. J. Wallentin, T. Wixe, O. F. Wendt, K. E. Bergquist, K. Wärnmark, *Chem. Eur. J.* **2010**, *16*, 3994 – 4002.

[6] a) A. J. Goshe, I. M. Steele, B. Bosnich, *J. Am. Chem. Soc.* **2003**, *125*, 444 – 451; b) J. D. Crowley, I. M. Steele, B. Bosnich, *Inorg. Chem.* **2005**, *44*, 2989 – 2991; c) J. D. Crowley, B. Bosnich, *Eur. J. Inorg. Chem.* **2005**, 2015 – 2025.

[7] a) D. Sun, F. S. Tham, C. A. Reed, L. Chaker, M. Burgess, P. D. W. Boyd, *J. Am. Chem. Soc.* **2000**, *122*, 10704 – 10705; b) Z. Q. Wu, X. B. Shao, C. Li, J. L. Hou, K. Wang, X. K. Jiang, Z. T. Li, *J. Am. Chem. Soc.* **2005**, *127*, 17460 – 17468.

[8] F. Wang, K. Matsuda, A. F. M. M. Rahman, X. Peng, T. Kimura, N. Komatsu, *J. Am. Chem. Soc.* **2010**, *132*, 10876 – 10881.

[9] J. Wu, F. Fang, W. Y. Lu, J. L. Hou, C. Li, Z. Q. Wu, X. K. Jiang, Z. T. Li, Y. H. Yu, *J. Org. Chem.* **2007**, *72*, 2897 – 2905.

[10] a) F. G. Klärner, B. Kahlert, R. Boese, D. Bläser, A. Juris, F. Marchioni, *Chem. Eur. J.* **2005**, *11*, 3363 – 3374; b) F. G. Klärner, B. Kahlert, *Acc. Chem. Res.* **2003**, *36*, 919 – 932.

[11] a) J. N. H. Reek, H. Engelkamp, A. E. Rowan, J. A. A. W. Elemans, R. J. M. Nolte, *Chem. Eur. J.* **1998**, *4*, 716 – 722; b) H. Kurebayashi, T. Haino, S. Usui, Y. Fukazawa, *Tetrahedron* **2001**, *57*, 8667 – 8674; c) T. Nishiuchi, Y. Kuwatani, T. Nishinaga, M. Iyoda, *Chem. Eur. J.* **2009**, *15*, 6838 – 6847; d) L. P. Hernández-Eguía, R. J. Brea, L. Castedo, P. Ballester, J. R. Granja, *Chem. Eur. J.* **2011**, *17*, 1220 – 1229.

[12] a) H. Kai, S. Nara, K. Kinbara, T. Aida, *J. Am. Chem. Soc.* **2008**, *130*, 6725 – 6727; b) T. Muraoka, K. Kinbara, T. Aida, *Nature* **2006**, *440*, 512 – 515.

[13] J.-M. Lehn, *Chem. Soc. Rev.* **2007**, *36*, 151 – 160.

[14] a) A. Petitjean, R. G. Khoury, N. Kyritsakas, J.-M. Lehn, *J. Am. Chem. Soc.* **2004**, *126*, 6637 – 6647; b) M. Barboiu, L. Prodi, M. Montalti, N. Zaccheroni, N. Kyritsakas, J.-M. Lehn, *Chem. Eur. J.* **2004**, *10*, 2953 – 2959; c) A. Petitjean, J.-M. Lehn, *Inorg. Chim. Acta* **2007**, *360*, 849 – 856; d) S. Ulrich, J.-M. Lehn, *Chem. Eur. J.* **2009**, *15*, 5640 – 5645; e) S. Ulrich, A. Petitjean, J.-M. Lehn, *Eur. J. Inorg. Chem.* **2010**, 1913 – 1928.

[15] C. H. Lee, H. Yoon, W. D. Jang, *Chem. Eur. J.* **2009**, *15*, 9972 – 9976.

[16] A. Iordache, M. Retegan, F. Thomas, G. Royal, E. Saint-Aman, C. Bucher, *Chem. Eur. J.* **2012**, *18*, 7648 – 7653.

[17] J. Leblond, H. Gao, A. Petitjean, J. C. Leroux, *J. Am. Chem. Soc.* **2010**, *132*, 8544 – 8545.

[18] Y. Suzaki, Y. Tsuchido, K. Osakada, *Tetrahedron Lett.* **2011**, *52*, 3883 – 3885.

[19] X. Zhang, J. Fu, T. G. Zhan, L. Dai, Y. Chen, X. Zhao, *Tetrahedron Lett.* **2013**, *54*, 5039 – 5042.

[20] H. Suezawa, T. Yoshida, Y. Umezawa, S. Tsuboyama, M. Nishio, *Eur. J. Inorg. Chem.* **2002**, 3148 – 3155.

[21] a) Y. Tanaka, K. M. C. Wong, V. W. W. Yam, *Chem. Sci.* **2012**, *3*, 1185 – 1191; b) Y. Tanaka, K. M. C. Wong, V. W. W. Yam, *Chem. Eur. J.* **2013**, *19*, 390 – 399; c) Y. Tanaka, K. M. C. Wong, V. W. W. Yam, *Angew. Chem.* **2013**, *125*, 14367 – 14370; *Angew. Chem. Int. Ed.* **2013**, *52*, 14117 – 14120.

[22] G. J. Stueber, M. Kieninger, H. Schettler, W. Busch, B. Goeller, J. Franke, H. E. A. Kramer, H. Hoier, S. Henkel, P. Fischer, H. Port, T. Hirsch, G. Rytz, J. L. Birbaum, *J. Phys. Chem.* **1995**, *99*, 10097 – 10109.

[23] a) M. H. Lim, B. A. Wong, W. H. Pitcock, Jr., D. Mokshagundam, M. H. Baik, S. J. Lippard, *J. Am. Chem. Soc.* **2006**, *128*, 14364 – 14373; b) R. Kumar, T. Guchhait, G. Mani, *Inorg. Chem.* **2012**, *51*, 9029 – 9038; c) C. H. Lee, J. S. Lee, H. K. Na, D. W. Yoon, H. Miyaji, W. S. Cho, J. L. Sessler, *J. Org. Chem.* **2005**, *70*, 2067 – 2074.

[24] a) J. Iwasa, K. Ono, M. Fujita, M. Akita, M. Yoshizawa, *Chem. Commun.* **2009**, 5746 – 5748; b) A. P. de Silva, D. B. Fox, A. J. M. Huxley, T. S. Moody, *Coord. Chem. Rev.* **2000**, *205*, 41 – 57; c) A. P. de Silva, H. Q. N. Gunaratne, T. Gunnlaugsson, A. J. M. Huxley, C. P. McCoy, J. T. Rademacher, T. E. Rice, *Chem. Rev.* **1997**, *97*, 1515 – 1566.

[25] M. Hyacinth, M. Chruszcz, K. S. Lee, M. Sabat, G. Gao, L. Pu, *Angew. Chem.* **2006**, *118*, 5484 – 5486; *Angew. Chem. Int. Ed.* **2006**, *45*, 5358 – 5360.

[26] M. Mosrin, P. Knochel, *Chem. Eur. J.* **2009**, *15*, 1468 – 1477.

[27] V. Percec, M. R. Imam, M. Peterca, D. A. Wilson, R. Graf, H. W. Spiess, V. S. K. Balagurusamy, P. A. Heiney, *J. Am. Chem. Soc.* **2009**, *131*, 7662 – 7677.

[28] Gaussian 09, Revision B.01, M. J. Frisch, G. W. Trucks, H. B. Schlegel, G. E. Scuseria, M. A. Robb, J. R. Cheeseman, G. Scalmani, V. Barone, B. Mennucci, G. A. Petersson, H. Nakatsuji, M. Caricato, X. Li, H. P. Hratchian, A. F. Izmaylov, J. Bloino, G. Zheng, J. L. Sonnenberg, M. Hada, M. Ehara, K. Toyota, R. Fukuda, J. Hasegawa, M. Ishida, T. Nakajima, Y. Honda, O. Kitao, H. Nakai, T. Vreven, J. A. Montgomery, Jr., J. E. Peralta, F. Ogliaro, M. Bearpark, J. J. Heyd, E. Brothers, K. N. Kudin, V. N. Staroverov, R. Kobayashi, J. Normand, K. Raghavachari, A. Rendell, J. C. Burant, S. S. Iyengar, J. Tomasi, M. Cossi, N. Rega, J. M. Millam, M. Klene, J. E. Knox, J. B. Cross, V. Bakken, C. Adamo, J. Jaramillo, R. Gomperts, R. E. Stratmann, O. Yazyev, A. J. Austin, R. Cammi, C. Pomelli, J. W. Ochterski, R. L. Martin, K. Morokuma, V. G. Zakrzewski, G. A. Voth, P. Salvador, J. J. Dannenberg, S. Dapprich, A. D. Daniels, Ö. Farkas, J. B. Foresman, J. V. Ortiz, J. Cioslowski, D. J. Fox, Gaussian, Inc., Wallingford CT, 2009.

[29] a) M. W. Schmidt, K. K. Baldridge, J. A. Boatz, S. T. Elbert, M. S. Gordon, J. H. Jensen, S. Koseki, N. Matsunaga, K. A. Nguyen, S. Su, T. L. Windus, M. Dupuis, J. A. Montgomery, *J. Comput. Chem.* **1993**, *14*, 1347 – 1363; b) M. S. Gordon, M. W. Schmidt in *Theory and Applications of Computational Chemistry: The First Forty Years* (Eds.: C. E. Dykstra, G. Frenking, K. S. Kim, G. E. Scuseria), Elsevier, Amsterdam, **2005**, pp. 1167 – 1189.

Received: November 10, 2013
Published online on March 6, 2014